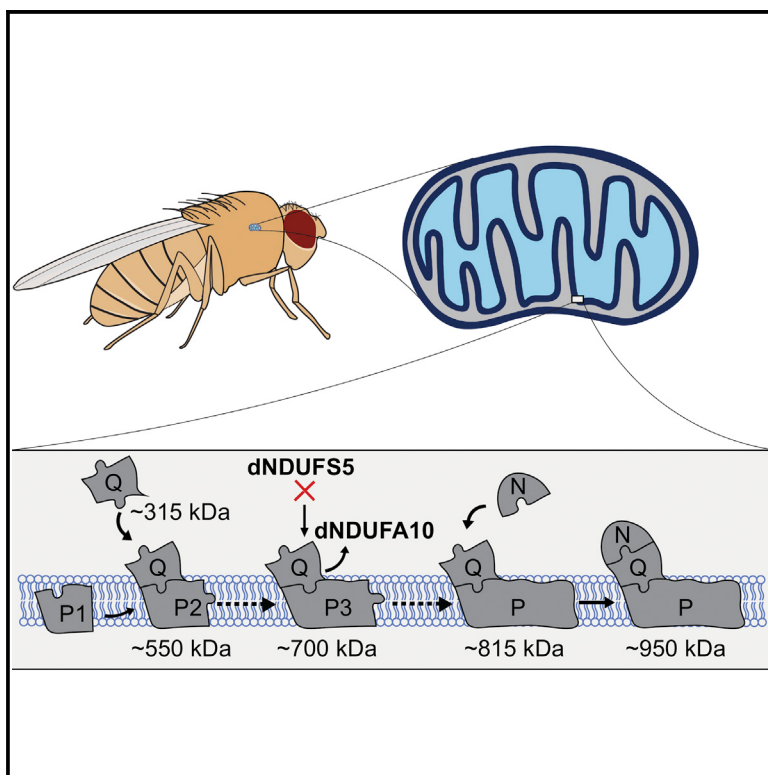


Regulation of Mitochondrial Complex I Biogenesis in *Drosophila* Flight Muscles

Graphical Abstract



Authors

Christian Joel Garcia, Jahan Khajeh, Emmanuel Coulanges, Emily I-ju Chen, Edward Owusu-Ansah

Correspondence

eo2364@cumc.columbia.edu

In Brief

Garcia et al. establish *Drosophila* as a suitable resource for studying mitochondrial complex I biogenesis. They find that at least 42 of the 44 distinct human complex I subunits are conserved in *Drosophila*, and many of these subunits have specific roles in complex I assembly *in vivo*.

Highlights

- Mitochondrial complex I (CI) biogenesis can be studied in *Drosophila* flight muscles
- Subcomplexes of ~315, ~550, and ~815 kDa are formed during CI assembly in *Drosophila*
- dNDUFS5 is required for converting an ~700 kDa subcomplex into the ~815 kDa subcomplex
- dNDUFS5 is required to stabilize or promote incorporation of dNDUFA10 into the complex



Regulation of Mitochondrial Complex I Biogenesis in *Drosophila* Flight Muscles

Christian Joel Garcia,^{1,4} Jahan Khajeh,^{1,4} Emmanuel Coulanges,¹ Emily I-ju Chen,² and Edward Owusu-Ansah^{1,3,5,*}

¹Department of Physiology and Cellular Biophysics

²Proteomics Shared Resource at the Herbert Irving Comprehensive Cancer Center and Department of Pharmacology

³The Robert N. Butler Columbia Aging Center

Columbia University Medical Center, New York, NY 10032, USA

⁴These authors contributed equally

⁵Lead Contact

*Correspondence: eo2364@cumc.columbia.edu

<http://dx.doi.org/10.1016/j.celrep.2017.06.015>

SUMMARY

The flight muscles of *Drosophila* are highly enriched with mitochondria, but the mechanism by which mitochondrial complex I (CI) is assembled in this tissue has not been described. We report the mechanism of CI biogenesis in *Drosophila* flight muscles and show that it proceeds via the formation of ~315, ~550, and ~815 kDa CI assembly intermediates. Additionally, we define specific roles for several CI subunits in the assembly process. In particular, we show that dNDUFS5 is required for converting an ~700 kDa transient CI assembly intermediate into the ~815 kDa assembly intermediate. Importantly, incorporation of dNDUFS5 into CI is necessary to stabilize or promote incorporation of dNDUFA10 into the complex. Our findings highlight the potential of studies of CI biogenesis in *Drosophila* to uncover the mechanism of CI assembly *in vivo* and establish *Drosophila* as a suitable model organism and resource for addressing questions relevant to CI biogenesis in humans.

INTRODUCTION

Mitochondrial complex I (CI) (NADH: ubiquinone oxidoreductase) is the first and largest of the electron transport chain complexes in the mitochondrion and has a molecular mass approaching 1 MDa (reviewed in Hirst, 2013). Human CI has 44 distinct subunits (Table S1), 14 of which are directly involved in transferring electrons from NADH to ubiquinone or in generation of the membrane potential. Because these 14 subunits are conserved from bacteria to humans and form the catalytic centers of the enzyme, they are referred to as the core or central subunits. The 30 remaining subunits are referred to as accessory or supernumerary subunits because they are not directly involved in catalysis and are expressed to varying extents among eukaryotes (Table S1) (reviewed in Hirst, 2013). A current hypothesis is that the accessory subunits may regulate reactive oxygen species (ROS) formation, complex assembly or stability, and cellular

homeostasis *in vivo*. Of note, disease-causing mutations in several accessory subunits have been identified (Berger et al., 2008; Budde et al., 2000; Hoefs et al., 2008, 2011; Kirby et al., 2004; Ostergaard et al., 2011; Scacco et al., 2003), and genetic disruption of some accessory subunits in cell lines impairs CI assembly (Guerrero-Castillo et al., 2017; Stroud et al., 2016). However, a definitive role for many of the accessory subunits *in vivo* remains to be established.

CI has two major arms: a hydrophobic membrane arm and a hydrophilic peripheral arm that juts into the mitochondrial matrix. The two arms are oriented almost perpendicularly to each other, resulting in a characteristic boot or L-shaped structure (Clason et al., 2010; Efremov et al., 2010; Radermacher et al., 2006; Zickermann et al., 2015). Several cryoelectron microscopy density maps and higher resolution atomic structures of CI from various eukaryotes have recently been described (Fiedorczuk et al., 2016; Vinothkumar et al., 2014; Zhu et al., 2016; Zickermann et al., 2015). The accessory subunits were found to form a cage around the core subunits and were particularly concentrated around the membrane domain. These observations lend further credence to the hypothesis that the accessory subunits may be involved in stabilizing the complex during or after biogenesis *in vivo*.

Surprisingly, despite the outstanding genetic capabilities of *Drosophila*, a systematic genetic analysis of CI assembly has not been described in this organism. Instead, previous *in vivo* genetic analyses of the regulation of eukaryotic CI assembly have been performed, primarily in the aerobic fungus *Neurospora crassa* (Duarte et al., 1995). Although the *N. crassa* model of CI assembly is renowned for being the first system for which a model of CI assembly was described, there are notable deviations from the assembly pathway in mammalian systems (Nehls et al., 1992; Tuschens et al., 1990). Thus, it is important to develop additional genetically tractable CI assembly model systems that more closely resemble and recapitulate the human system. Importantly, *Drosophila* has a comparable number of CI subunits (similar to the human and bovine enzymes) and more than a dozen putative assembly factors, all of which have clear human orthologs, making it a suitable model organism for studying CI assembly. Studying CI assembly in *Drosophila* has the added advantage of being in an *in vivo* context, in which the effects of both developmental signals and environmental perturbations can be examined. Accordingly,

we have analyzed the role of several nuclear-encoded CI subunits in CI assembly in *Drosophila* muscles.

We describe the mechanism of CI assembly in *Drosophila* flight muscles. Specifically, we show that many of the accessory subunits regulate specific stages of CI biogenesis in vivo, such that when their levels of expression are reduced, CI activity is diminished because of impaired CI assembly. We demonstrate that CI biogenesis in *Drosophila* involves the formation of ~315, ~550, and ~815 kDa assembly intermediates, and that RNAi-mediated knockdown of either dNDUFS2 or dNDUFS3 decreases the amount of the ~315 kDa assembly intermediate that is formed. Furthermore, we show that a specific accessory subunit, dNDUFA5, is required for the formation and/or stabilization of the ~315 kDa assembly intermediate in vivo. Additionally, we define a specific role for another accessory subunit (dNDUFS5) and show that it is required for converting a transient CI assembly intermediate (an ~700 kDa assembly intermediate) into the ~815 kDa assembly intermediate, during one of the terminal steps of CI assembly. Four components of the mitochondrial CI assembly (MCIA) complex (dECSIT, dNDUFAF1, dACAD9, and dTIMMDC1) are associated with the ~700 kDa assembly intermediate, further confirming that it is a true assembly intermediate in CI biogenesis. Importantly, incorporation of dNDUFS5 into CI is necessary to stabilize or promote incorporation of dNDUFA10 into the complex. We also identify several roles for many of the dNDUFB subunits. Altogether, our analyses reveal how studies of CI biogenesis in *Drosophila* can uncover mechanisms of CI assembly in vivo and establish *Drosophila* as an important genetically pliable model organism for addressing questions relevant to mammalian CI biogenesis.

RESULTS

Drosophila Flight Muscles Are Suitable for Studying CI Assembly

CI consists of a hydrophilic matrix arm and a hydrophobic membrane arm that are oriented almost orthogonally to each other (Figure 1A). Subunits with the prefix NDUFA (NDUFA1-3 and NDUFA5-13) were so named as they were originally thought to be part of the matrix arm, whereas the NDUFB subunits (NDUFB1-NDUFB11) are part of the membrane arm. In addition, subunits that are found in the vicinity of the eight Fe-S clusters (NDUFS) or single flavoprotein (NDUFV) are also localized in the matrix. All the NDUFA and NDUFB subunits are accessory subunits (Figure 1A). We used the *Drosophila* RNAi Screening Center Integrative Ortholog Prediction Tool (DIOPT) to identify 42 putative orthologs of the 44 human CI subunits (Figure 1B; Table S1) (Hu et al., 2011). To facilitate comparison with their human orthologs, in this paper we refer to *Drosophila* orthologs of the human CI subunits as dNDUFS1, dNDUFS2, and so on. Their designated gene nomenclature in *Drosophila* is shown in Table S1.

To confirm whether the putative CI orthologs identified by DIOPT were bona fide CI subunits in *Drosophila* flight muscles, we isolated mitochondria from thoraxes of wild-type flies, solubilized their membranes in 1% digitonin, and resolved their oxidative phosphorylation (OXPHOS) complexes into various bands using blue native PAGE (BN-PAGE) (Rera et al., 2011; Wittig et al., 2006). We solubilized the mitochondrial membranes in

1% digitonin because we found that 1% digitonin was the optimal detergent concentration for isolating and resolving OXPHOS complexes in their native state in *Drosophila* (Figure S1), as has been reported previously (Rera et al., 2011; Wittig et al., 2006). Subsequently, we cut out each of the bands detected by Coomassie staining of the gel and identified their composition by mass spectrometry (Figure 1C). We confirmed the existence of 37 of the 42 putative CI orthologs on the basis of their presence in the band corresponding to the CI holoenzyme (band B) and/or supercomplex (band A) (Figure 1C; Tables S1 and S2). Notably, the *Drosophila* ortholog of NDUFA4 (ND-MNLL), a protein that was previously considered a CI subunit but has been reassigned as a complex IV (CIV) subunit (Balsa et al., 2012), co-migrated with the CIV band (band E) (Figure 1C; Table S2). In addition, four of the subunits we were unable to detect are highly hydrophobic membrane-embedded core subunits encoded in the mitochondrion (ND2, ND3, ND4L, and ND6); thus they may have escaped detection because of their highly hydrophobic nature. Interestingly, these subunits were not identified in a previous proteomic analysis of CI in mouse cell lines (Balsa et al., 2012).

Coomassie- or silver-stained native gels containing mitochondrial protein complexes from flies expressing RNAi to CI, complex III (CIII), CIV, and complex V (CV) proteins further confirmed the identities of the bands cut for mass spectrometry (Figure 1D). Because our mass spectrometry data suggested that a portion of CI might be co-migrating with CV and possibly CIII, we tested whether this co-migration was the result of supercomplex formation. We were unable to find antibodies that cross-react with any of the *Drosophila* CIII proteins, but antibodies that cross-react with dNDUFS3 (a CI protein) and dATPSyn β (a CV protein) were commercially available and were used to examine the identity of “band A” via western blotting. As is evident in the silver staining gel (Figure 1D), immunoblotting revealed that “band A” was actually a doublet, and the lower band in the doublet corresponds to a dimer of CV, as has been observed in other contexts (Figure 1E) (Rera et al., 2011; Wittig et al., 2006). In addition, CI in flight muscles was found to exist predominantly as the holoenzyme, with a relatively small portion involved in CI-CIII supercomplex formation, which migrates as an upper band in the doublet (Figure 1E). Notably, the observation that CI in *Drosophila* flight and skeletal muscles occurs predominantly as the holoenzyme (i.e., free CI, not involved in supercomplex formation) contrasts markedly with CI in cardiac or skeletal muscles from mice, in which a significant portion of CI is trapped in supercomplex formation (Figure 1F). Thus, in addition to the genetic capabilities of *Drosophila*, and the fact that it has a comparable number of CI subunits as the human enzyme, it is a suitable model for studying CI assembly because most CI in flight muscles exists as the holoenzyme. Accordingly, a defect in CI biogenesis can easily be scored and quantified. Consequently, we decided to examine the role of the nuclear-encoded CI subunits in CI assembly.

Disruption of Several CI Subunits in Flight Muscles Impairs CI Assembly

We found that loss-of-function alleles for many *Drosophila* CI genes are lethal (not shown). Therefore, to ascertain which CI

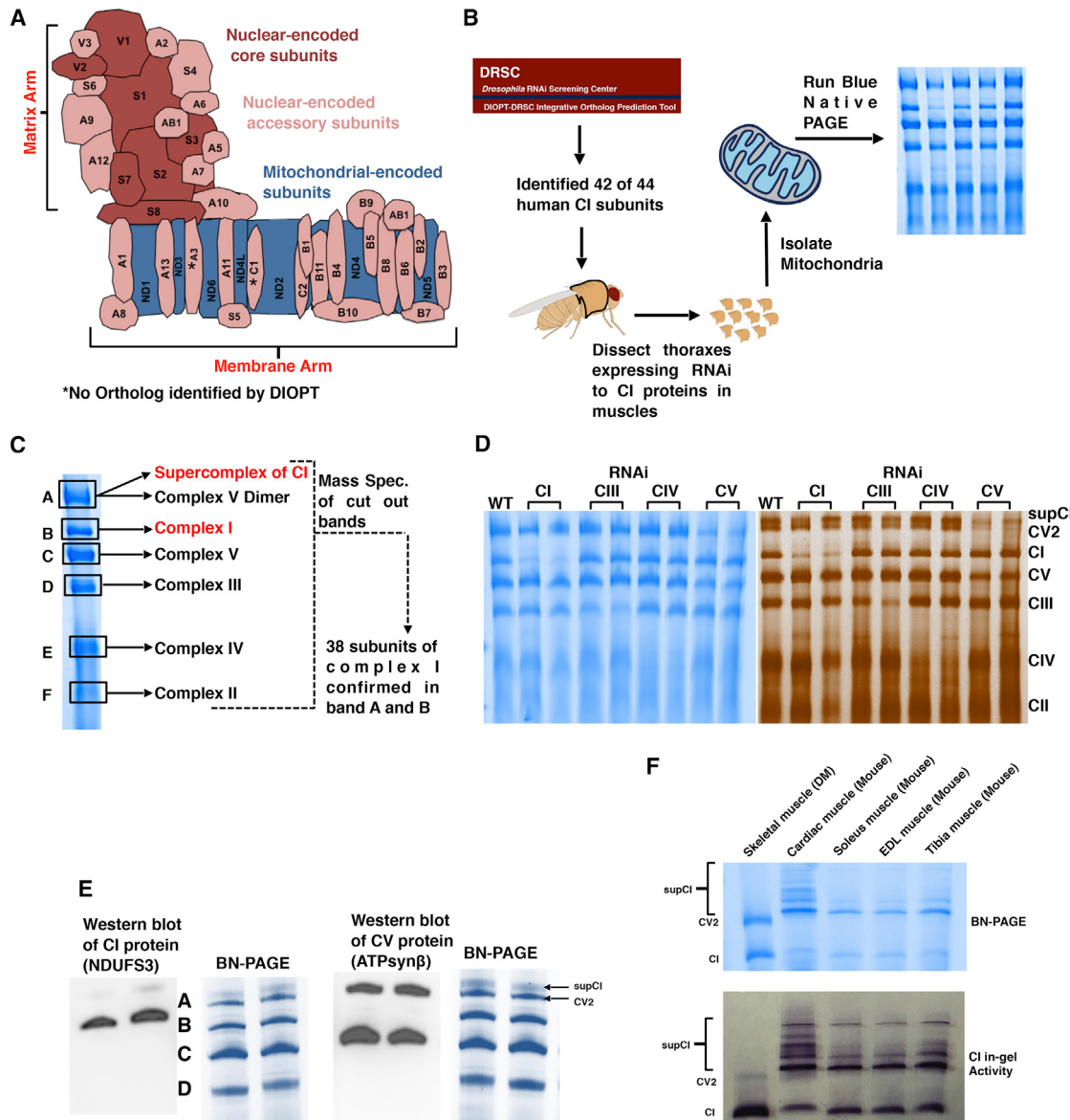


Figure 1. *Drosophila* Flight Muscles Are Suitable for Studying Complex I Assembly

(A) Schematic representation of how the 44 distinct subunits of bovine or ovine CI are arranged to produce the L-shaped topology; based on recent CI structures described (Fiedorczuk et al., 2016; Vinothkumar et al., 2014; Zhu et al., 2016; Zickermann et al., 2015). The asterisk denotes subunits for which an ortholog was not identified in *Drosophila* by DIOPT. NDUFAB1 occurs twice in the complex, giving rise to a total of 45 subunits.

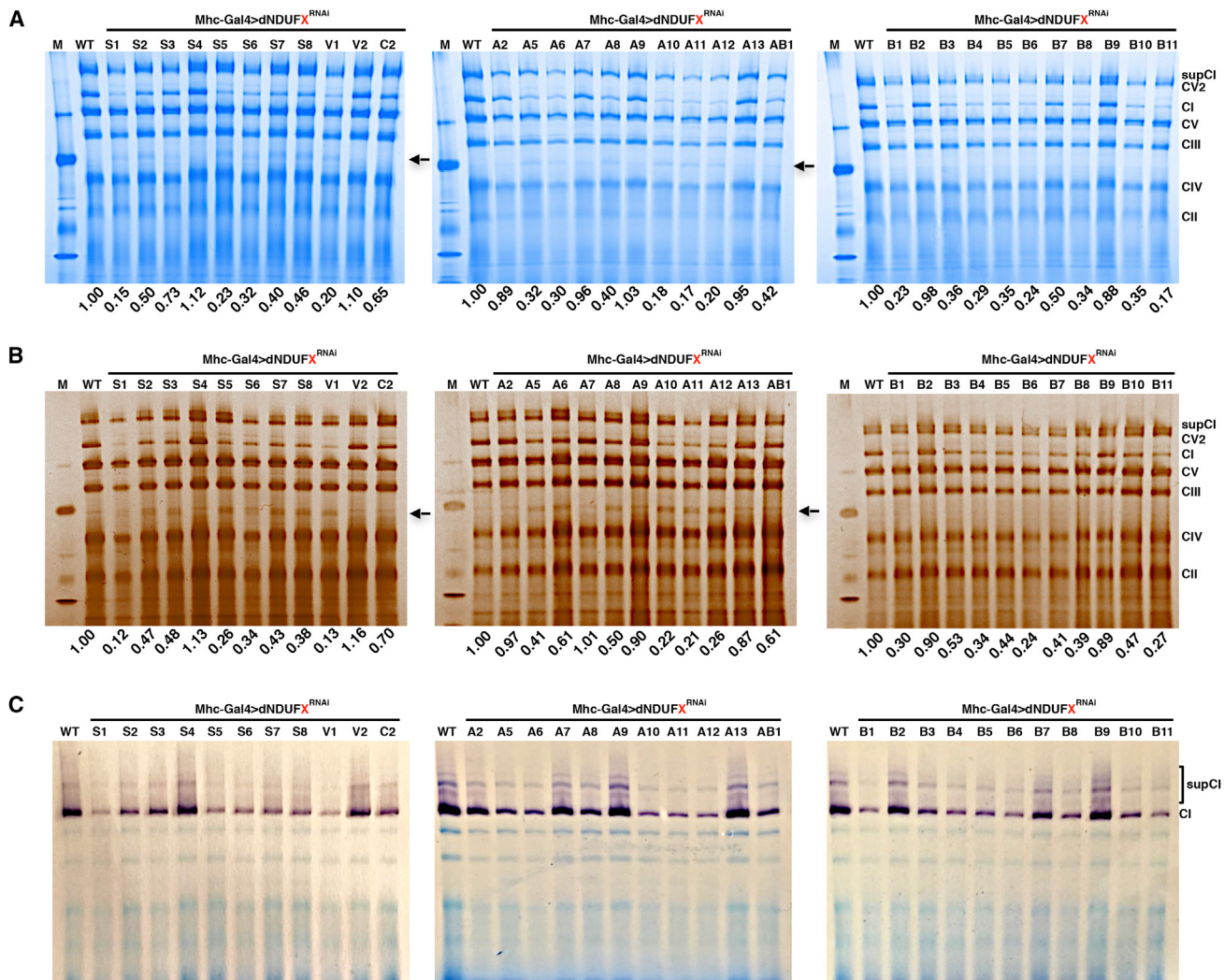
(B) Summary of the experimental procedure for studying CI assembly in *Drosophila*. Transgenic RNAi constructs to the nuclear-encoded subunits were expressed specifically in thoracic muscles using the *mhc-Gal4* driver. Mitochondria were isolated from thoraxes of 1-week-old flies, solubilized in 1% digitonin, and analyzed by blue native PAGE (BN-PAGE).

(C) The constituents of each of the six major bands observed during BN-PAGE was analyzed by MS. Thirty-eight subunits of *Drosophila* CI were confirmed by MS. The 38 subunits correspond to 37 different orthologs of human CI. Two paralogs of human NDUFV1 were confirmed by MS (see Table S1). See Table S2 for all the peptides identified in the six major bands shown.

(D) BN-PAGE (left) and silver staining (right) of samples from thoraxes following RNAi-mediated knockdown of complex I (CI), complex III (CIII), complex IV (CIV), and complex V (CV) proteins to confirm the identities of the bands. SupCI and CV2 denote a supercomplex of CI and a dimer of CV, respectively. The exact RNAi constructs expressed starting from left to right were to the white gene (wild-type [WT]), dNDUFV1 (CI), dNDUFS1 (CI), dUQCRC-2 (CIII), dUQCRC-Q (CIII), dCox5A (CIV), cyclope (CIV), dATPsyn- β (CV), and ATPsyn- β (CV).

(E) Immunoblotting with anti-NDUFS3 and anti-ATPsyn β antibodies of native gels to detect CI and CV, respectively. Note that band A is a doublet consisting predominantly of a dimer of CV and a supercomplex of CI.

(F) BN-PAGE (top) and CI in-gel enzyme activity (bottom) indicate that most of CI exists as the holoenzyme in *Drosophila melanogaster* (DM) skeletal muscles, in contrast to cardiac, soleus, extensor digitorum longus (EDL), and tibia muscles from mice where a significant portion of CI exists as a supercomplex.

**Figure 2. Disruption of Several CI Core and Supernumerary Subunits Impairs CI Assembly in *Drosophila***

(A) BN-PAGE, (B) silver staining, and (C) CI in-gel enzyme activity of mitochondria isolated from thoraxes following RNAi-mediated knockdown of the CI proteins indicated (*mhc-Gal4>dNDUFX^{RNAi}*). The values listed below each lane indicate the residual amount of CI normalized to the amount in the wild-type (*mhc-Gal4>w¹¹¹⁸*) lane.

subunits are required for CI biogenesis in *Drosophila*, we used the Gal4/UAS system to express transgenic RNAi constructs (henceforth referred to as UAS-RNAi lines) to both core and accessory CI subunits (Brand and Perrimon, 1993). We examined the effect of knocking down the subunits specifically in muscles (using either *Dmef2-Gal4* or *mhc-Gal4*). Transgenic expression of many of the UAS-RNAi constructs using *Dmef2-Gal4*, a muscle-restricted Gal4 driver that is expressed strongly throughout development, caused lethality (not shown). However, a genetic cross between each of the UAS-RNAi lines and *mhc-Gal4* produced viable flies, as the *mhc-Gal4* driver has a weaker expression relative to *Dmef2-Gal4* during the initial larval stages (Figure S2). Accordingly, we decided to analyze CI assembly in mitochondria isolated from thoraxes of *mhc-Gal4/UAS-CI^{RNAi}* flies (henceforth referred to as *mhc>CI^{RNAi}* flies) using BN-PAGE.

We observed that in general, both core and accessory subunits produced CI assembly defects whenever the extent of transcript knockdown was more than 50% (Figure 2A). To further assess the extent of the CI assembly deficit for each subunit, we quantified the amount of CI relative to the amount of CV in each lane and normalized it to the corresponding value in the wild-type lane. Interestingly, this revealed that some of the most robust CI assembly deficits were observed when accessory or supernumerary subunits (such as dNDUFA10–12 and dNDUFB4–6) were genetically impaired (Figures 2A and 2B). Similar results were obtained with silver staining of the protein complexes in the native gels (Figure 2B). Finally, in-gel CI enzyme activity assay revealed that the assembly deficits correlated with a reduction in CI activity (Figure 2C). Altogether, these results indicate that many of the core and accessory subunits are essential for viability and biogenesis of the CI holoenzyme or

supercomplex in flight muscles. Accordingly, we turned our attention toward elucidating the mechanism of CI assembly in *Drosophila* flight muscles.

Proteomic Analyses and Immunoblotting Identify Assembly Intermediates of CI

Studies from some mammalian cell lines have shown that CI biogenesis proceeds via a series of assembly intermediates that combine with each other, or other subunits, to form the ~950 kDa boot-shaped holoenzyme. The assembly intermediates generally correspond to partial or complete domains of the three functional modules of CI. The NADH dehydrogenase module (N module) is located at the tip of the matrix arm and is the site of NADH oxidation. Situated between the N module and the membrane is the Q module, which is responsible for ubiquinone reduction. The proton-conducting P module in the membrane arm can be subdivided into a proximal P_p module (roughly corresponding to the first half of the P module that connects with the Q module) and a distal P_d module (Figure 3A).

The current model posits that CI assembly in mammalian systems begins with the formation of a small assembly intermediate containing NDUFS2 and NDUFS3, which combines with NDUFS7 and NDUFS8 (Figure 3B). This assembly intermediate is the primary component of the Q module and ultimately combines with ND1 to form an ~315 kDa assembly intermediate that is anchored to the mitochondrial inner membrane. The ~315 kDa assembly intermediate combines with an independently formed ~370 kDa assembly intermediate to form an ~550 kDa assembly intermediate (Figure 3B). The ~550 kDa assembly intermediate, which consists of the complete Q module and a portion of the P module, grows by the addition of more subunits to form the ~815 kDa assembly intermediate, via mechanisms that are very poorly defined. At this point, the ~815 kDa assembly intermediate is generally considered to be composed of the complete Q and P modules. Finally, an independently formed assembly intermediate consisting of NDUFS1, NDUFV1, NDUFV2, NDUFV3, NDUFS4, NDUFS6, and NDUFA12, which together form the N module, is added as a “cap” to the ~815 kDa assembly intermediate to produce the ~950 kDa holoenzyme (Figure 3B; the ~315, ~370, ~550, and ~815 kDa assembly intermediates were previously estimated as ~400, ~460, ~650, and ~830 kDa subcomplexes, respectively; Andrews et al., 2013; Vartak et al., 2014).

Because some flight muscles are formed by 24 hr after pupal formation (Roy and VijayRaghavan, 1999), we decided to ascertain the extent of CI biogenesis starting at 48 hr (i.e., 2 days) post-pupariation. Specifically, we isolated mitochondria at various time points and examined CI assembly via western blotting of the native complexes. Because current models of mammalian CI assembly postulate that NDUFS3 and ND1 are both part of the ~815, ~550, and ~315 kDa assembly intermediates, western blot with anti-NDUFS3 or anti-ND1 antibodies will be expected to detect these three assembly intermediates and possibly lower molecular weight assembly intermediates (if the respective epitopes are not masked when the assembly intermediate is formed). In addition, the fully assembled CI and CI-containing supercomplexes will be expected to be detected as well.

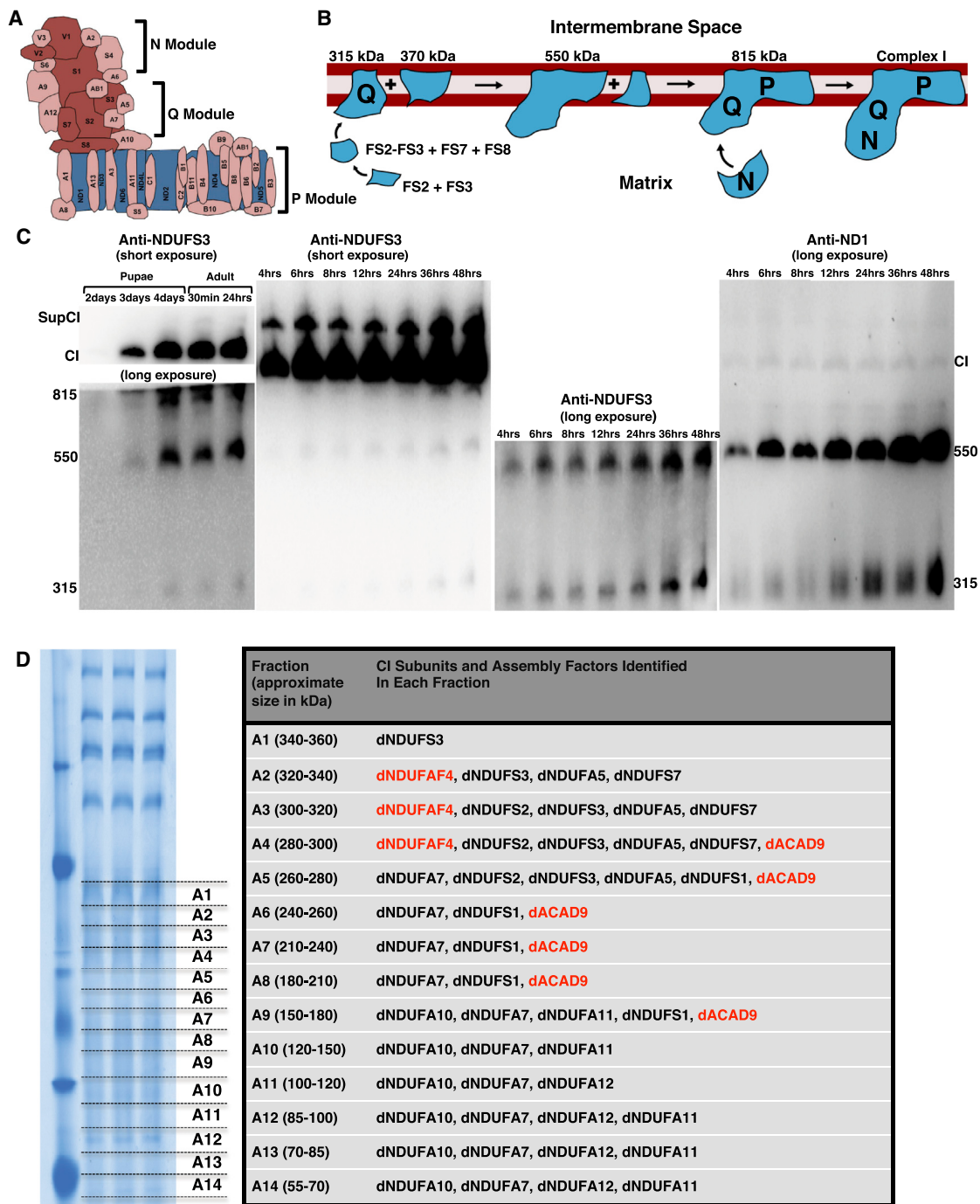
Indeed, immunoblotting with anti-NDUFS3 revealed that a portion of CI is assembled during pupal development and continues during the first 48 hr after flies eclose (emerge as adults from pupae) (Figure 3C). Although we were able to detect the ~315 and ~550 kDa assembly intermediates with the anti-ND1 antibody (Figure 3C), the higher molecular weight bands were only weakly detectable, conceivably because the epitope to which this antibody was raised for this hydrophobic subunit becomes less exposed to the aqueous environment during the final stages of CI biogenesis (Figure 3C). Moreover, although we were able to detect subcomplexes of CV that migrate with an apparent mass of about 100 kDa at this stage of development (Figure S3), we were unable to detect dNDUFS3-containing assembly intermediates with an apparent mass of less than 200 kDa. There are at least two possible explanations for this result: (1) the smaller NDUFS3-containing assembly intermediates may not be present at this stage, or (2) the epitope of dNDUFS3 in the smaller assembly intermediates was inaccessible to the antibody, perhaps as a result of being masked by bound assembly factors and/or other interactors. Therefore, we used proteomic analyses to distinguish between these two possibilities.

Mitochondria were isolated from thoraxes of wild-type flies that had been aged for 24 hr after eclosure and subjected to BN-PAGE. Subsequently, the region of the gel between ~50 and ~350 kDa was excised and divided into 14 slices (labeled fractions A1–A14) for in-gel digestion and subsequent proteomics analyses (Figure 3D). We observed that dNDUFS2, dNDUFS3, and dNDUFS7 co-migrated in fractions corresponding to a mass of approximately 280–320 kDa (Figure 3D; Table S3). Interestingly, the CI assembly factor, dNDUFAF4, was also found in these fractions (Figure 3D; Table S3). In addition, dNDUFA5 co-migrated with dNDUFS2, dNDUFS3, and dNDUFS7 (Figure 3D), confirming that it is a component of the ~315 kDa assembly intermediate in vivo. Importantly, although several other CI subunits migrated in fractions corresponding to a mass of approximately 50–250 kDa, neither dNDUFS2 nor dNDUFS3 was found in these fractions. Thus, it appears that in an in vivo context, in *Drosophila* flight muscles, the constituents of the ~315 kDa assembly intermediate are combined almost synchronously.

Specific Subunits Regulate the Biogenesis or Stability of Specific Assembly Intermediates of CI

If the assembly intermediates observed are bona fide intermediates in the pathway of CI assembly in *Drosophila*, then at least some of these assembly intermediates will stall and accumulate, or they may disintegrate when specific CI subunits that are required for CI assembly are disrupted (Figure 4A). To test this hypothesis, we analyzed the CI assembly intermediates from thoraxes of *Mhc>CI^{RNAi}* flies 24 hr after eclosure using an anti-NDUFS3 antibody. As expected, the various subunits that produced CI assembly deficits in Figure 2 also resulted in a reduction of the level of the holoenzyme or the CI-containing supercomplex (Figures 4B–4F).

Disruption of dNDUFS1 and dNDUFS1, which are components of the N module of CI and are thus expected to be added as part of the “cap” during the final step in CI assembly, resulted in a stalling and accumulation of the ~815 kDa assembly

**Figure 3. Proteomic Analyses and Immunoblotting Identify Assembly Intermediates of CI**

(A) Schematic of CI showing the three modules of the enzyme. The NADH dehydrogenase module (N module) is located at the tip of the matrix arm and is the site of NADH oxidation. Situated between the N module and the membrane arm is the Q module, which is responsible for ubiquinone reduction. The proton-conducting P module is in the membrane arm.

(B) The current model of CI assembly in mammalian systems (reviewed in Vartak et al., 2014). The assembly process begins with the formation of an assembly intermediate containing NDUFS2 and NDUFS3, which combines with NDUFS7 and NDUFS8. The subcomplex of NDUFS2, NDUFS3, NDUFS7, and NDUFS8 ultimately combines with ND1 to form the ~315 kDa assembly intermediate that is anchored to the membrane. The ~315 kDa subcomplex (also called the Q module) combines with an independently formed ~370 kDa assembly intermediate to form an ~550 kDa assembly intermediate. This assembly intermediate that consists of the Q module and part of the P module grows by the addition of more subunits to form the ~815 kDa assembly intermediate, via mechanisms that are very poorly defined. The ~815 kDa assembly intermediate now consists of the complete Q and P modules. Finally, the N module is added to produce the 950 kDa

(legend continued on next page)

intermediate (Figure 4B). However, unexpectedly, disruption of dNDUFA6 and dNDUFA12 also stalled the ~815 kDa subcomplex (Figure 4C). RNAi-mediated knockdown of dNDUFS2, dNDUFS3, dNDUFS5, dNDUFS7, and dNDUFS8 led to a reduction in the amount of the ~815 kDa assembly intermediate (relative to wild-type), as they impaired some of the initial steps of CI biogenesis (Figure 4B). In addition, the amount of the ~315 kDa assembly intermediate was drastically reduced when the expression of dNDUFS2, dNDUFS3, or dNDUFS7 was impaired (Figure 4B), in line with our proteomic results in Figure 3D and current mammalian CI assembly models that show that the first step in CI biogenesis involves the formation of an assembly intermediate consisting of NDUFS2 and NDUFS3 (Figure 3B) (reviewed in Vartak et al., 2014). Notably, we found that RNAi-mediated knockdown of dNDUFA5 depleted the ~315 kDa assembly intermediate (Figure 4C). Combining this result, with our proteomic data showing that dNDUFA5 co-migrates with dNDUFS2, dNDUFS3, and dNDUFS7 (Figure 3D), we conclude that although dNDUFA5 is an accessory subunit, it is a critical component of, and required for formation or stabilization of the ~315 kDa assembly intermediate (i.e., the Q module) *in vivo*.

Disruption of most of the dNDUFB subunits did not markedly alter the stability or extent of accretion of the CI assembly intermediates 24 hr after eclosion (Figure 4D), but by 48 and 72 hr after eclosion some notable and consistent phenotypes between the two time points were observed (Figures 4E and 4F). For instance, RNAi-mediated disruption of dNDUFB3 decreased the extent of accumulation of all the assembly intermediates, and the 550 kDa assembly intermediate accumulated when dNDUFB1, dNDUFB8, and dNDUFB11 were impaired at both time points (i.e., 48 and 72 hr post-eclosion). Surprisingly, although none of the NDUFB subunits are known to be part of the 315 kDa assembly intermediate, the extent of accumulation of the 315 kDa assembly intermediate was diminished when the expression of dNDUFB1, dNDUFB4, dNDUFB5, dNDUFB6, and dNDUFB10 were reduced (Figures 4E and 4F). Taken together, these results indicate that specific subunits regulate the biogenesis or stability of specific CI assembly intermediates during CI assembly in *Drosophila* thoraxes.

Identification of an ~700 kDa Assembly Intermediate of CI in *Drosophila*

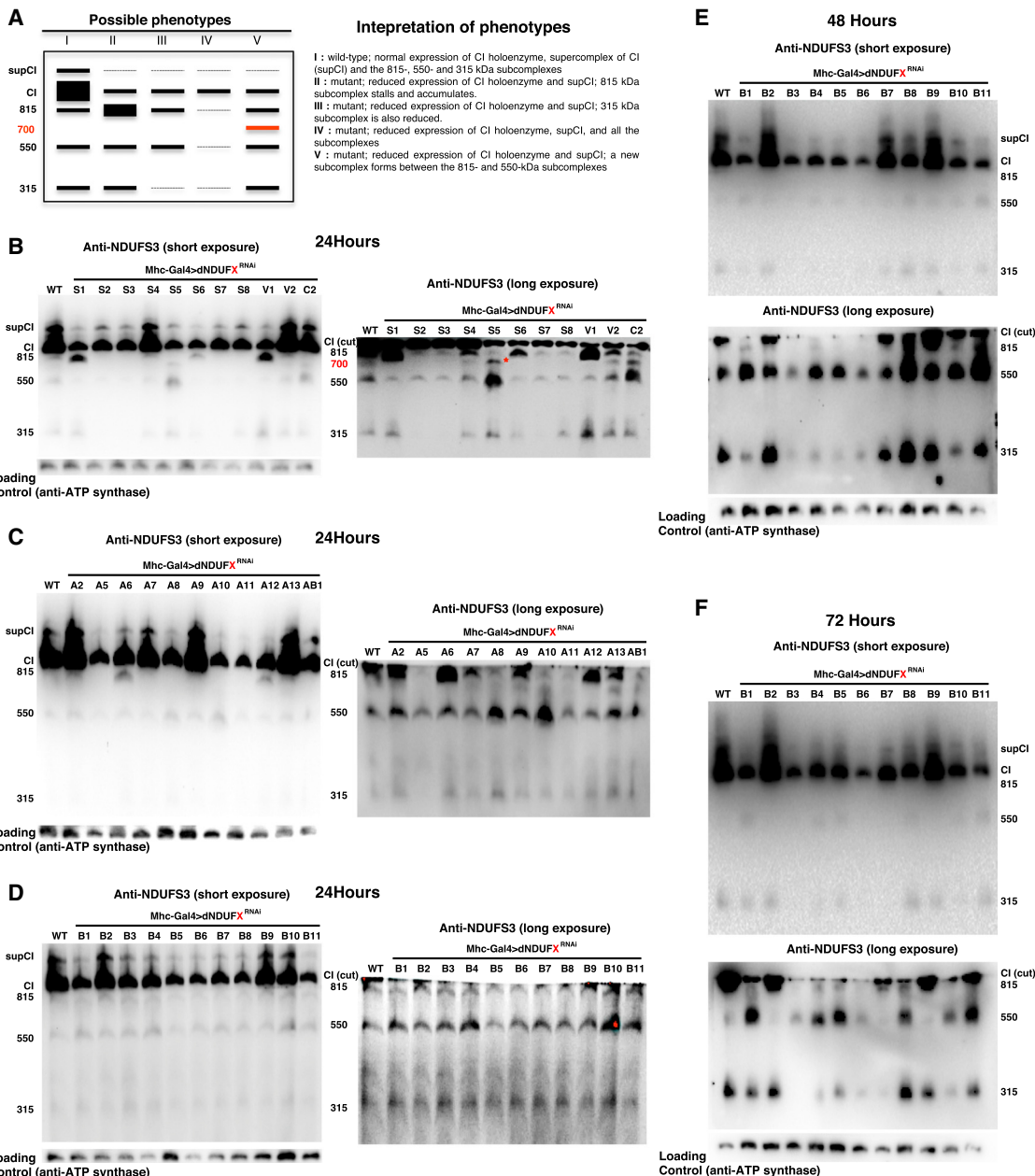
An assembly intermediate that accumulates between the ~550 and ~815 kDa assembly intermediates was detected on immunoblots of samples from *mhc>dNDUFS5^{RNAi}* and *mhc>dNDUFC2^{RNAi}* thoraxes (Figure 4B). We estimate its size to be ~700 kDa because it co-migrates with CV, previously

estimated to be ~700 kDa in blue native gels (Figure 5A) (Abdrakhmanova et al., 2006). The accumulation of the ~700 kDa assembly intermediate in samples from *mhc>dNDUFS5^{RNAi}* thoraxes was notable, because it suggested that this could be the point of entry of dNDUFS5 during CI assembly. NDUFS5 is a membrane-associated accessory subunit that extends into the intermembrane space; it is currently unclear at what point it becomes incorporated into CI. In contrast to the ~315, ~550, and ~815 kDa assembly intermediates, the ~700 kDa assembly intermediate was not readily perceptible by anti-NDUFS3 immunoblotting in the wild-type sample or most of the other mutant samples isolated 24 hr after eclosion (Figure 4B). This raised the possibility that it could simply be a degradation product, perhaps emanating from the ~815 kDa assembly intermediate.

To determine whether the ~700 kDa assembly intermediate is a true assembly intermediate, we decided to look at earlier time points (6 and 12 hr post-eclosion) to ascertain whether it ever appears in wild-type samples. Immunoblotting at these time points revealed that accumulation of the ~700 kDa assembly intermediate in *mhc>dNDUFS5^{RNAi}* thoraxes is present by the 6 hr time point and gradually tapers off afterward (Figure 5B). Importantly, at the 6 hr time point, a faint band corresponding to the ~700 kDa assembly intermediate can be observed in wild-type samples, indicating that the ~700 kDa assembly intermediate exists in wild-type samples and rapidly matures to the ~815 kDa assembly intermediate. The stalling of the ~700 kDa assembly intermediate in *mhc>dNDUFS5^{RNAi}* thoraxes occurred concurrently with an accumulation of both the ~550 and ~315 kDa assembly intermediates, and a diminution of the ~815 kDa assembly intermediate relative to wild-type levels. Thus, dNDUFS5 may be required for converting the ~700 kDa assembly intermediate into the ~815 kDa assembly intermediate, such that when this fails, there is a backlog of the ~700, ~550, and ~315 kDa assembly intermediates. To test this hypothesis, we compared the assembly intermediates that accumulate in *mhc>dNDUFS5^{RNAi}*, *dNDUFS1^{RNAi}* and *mhc>dNDUFS5^{RNAi}, dNDUFV1^{RNAi}* thoraxes with that in *mhc>dNDUFS1^{RNAi}* and *mhc>dNDUFV1^{RNAi}* thoraxes, respectively. We reasoned that because the ~815 kDa assembly intermediate accumulates in *mhc>dNDUFS1^{RNAi}* and *mhc>dNDUFV1^{RNAi}* thoraxes (Figure 4B), if dNDUFS5 is required for converting the ~700 kDa assembly intermediate into the ~815 kDa assembly intermediate, then the extent of accumulation of the ~815 kDa assembly intermediate in either *mhc>dNDUFS5^{RNAi}, dNDUFS1^{RNAi}* and/or *mhc>dNDUFS5^{RNAi}, *dNDUFV1^{RNAi}* thoraxes should be reduced relative to *mhc>dNDUFS1^{RNAi}* and *mhc>dNDUFV1^{RNAi}*, respectively. In agreement with this proposition, we observed that the accumulation of the ~815 kDa assembly intermediate was significantly*

fully assembled complex. Assembly factors or chaperones that assist in this process but are not present in the fully assembled complex have been omitted for clarity.

(C) Western blot of samples obtained from thoraces from pupae aged between 2 and 4 days after pupariation and of flies from 0.5 to 48 hr post-eclosion to detect the assembly intermediates, fully assembled CI, and a supercomplex containing complex I (supCI) after BN-PAGE. The anti-NDUFS3 antibody strongly detects CI and supCI and weakly detects the ~315, ~550, and ~815 kDa assembly intermediates after a short exposure. However, after a longer exposure, the ~315 and ~550 kDa assembly intermediates can clearly be seen. At right, the membrane was stripped and re-probed with anti-NDI. Anti-NDI detects the ~315 and ~550 kDa assembly intermediates and a very faint band corresponding to CI. (D) Proteomic analyses of assembly intermediates that form in the native gel sized between ~50 and ~350 kDa. See Table S3 for all the peptides identified.

**Figure 4. Specific Subunits Regulate the Biogenesis or Stability of Specific Assembly Intermediates of CI**

(A) Left: schematic of the distribution of assembly intermediates on immunoblots as a result of RNAi-mediated disruption of various CI subunits. Right: description of how various results can be interpreted.

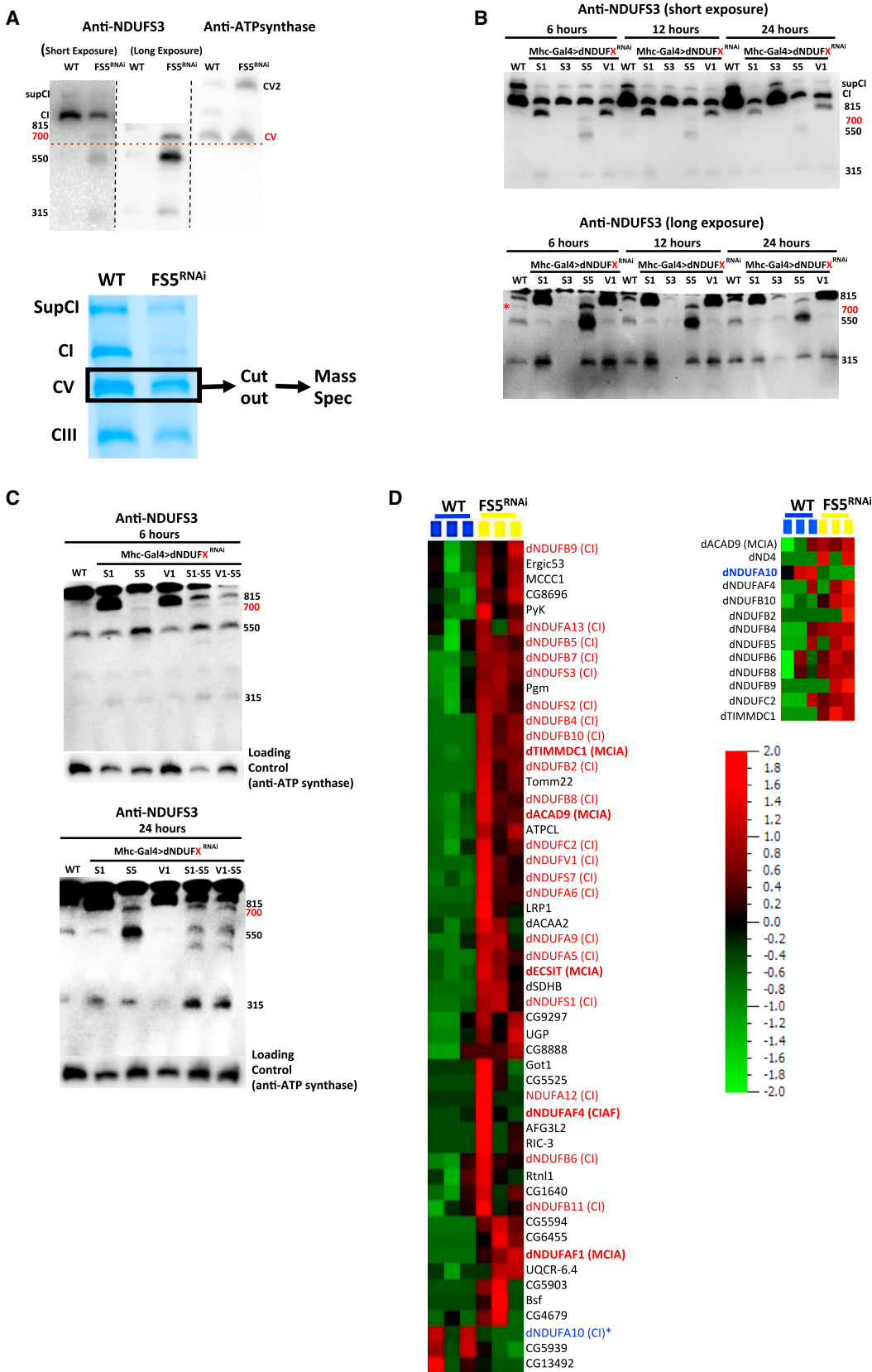
(B-D) Distribution of assembly intermediates in thoraxes dissected 24 hr after eclosion with transgenic RNAi expression of the CI subunits shown. In panels labeled "long exposure," the region of the membrane just at or below CI was cut and imaged.

(B) The ~815 kDa assembly intermediate accumulates in thoraxes expressing transgenic RNAi to dNDUFS1 and dNDUFV1; and the ~315 kDa assembly intermediate is decreased in thoraxes expressing transgenic RNAi of dNDUFS2, dNDUFS3, and dNDUF7. In addition, another assembly intermediate accumulates in thoraxes expressing RNAi to dNDUFS5 and dNDUFC2 (denoted by an asterisk).

(C) The ~815 kDa assembly intermediate stalls in thoraxes expressing transgenic RNAi to dNDUFA6 and dNDUFA12; and the ~315 kDa assembly intermediate is attenuated in thoraxes expressing transgenic RNAi of dNDUFA5.

(D) There were no overt alterations in assembly intermediates at this time point when the dNDUFB subunits were disrupted.

(E and F) Distribution of assembly intermediates in thoraxes dissected 48 hr (E) and 72 hr (F) after eclosion with transgenic RNAi expression of the NDUFB subunits shown. RNAi-mediated knockdown of the expression of dNDUFB3 decreased the extent of accumulation of all the assembly intermediates, and the 550 kDa assembly intermediate accumulated when the expression of dNDUFB1, dNDUFB8 and dNDUFB11 were reduced. In addition, the extent of accumulation of the 315 kDa assembly intermediate was diminished following RNAi-mediated disruption of dNDUFB1, dNDUFB4, dNDUFB5, dNDUFB6, and dNDUFB10 at both the 48 and 72 hr time points.



(legend on next page)

attenuated in *mhc>dNDUFS5^{RNAi},dNDUFS1^{RNAi}* thoraxes relative to *mhc>dNDUFS1^{RNAi}* thoraxes (Figure 5C). This was also accompanied by an accumulation of the ~700 kDa assembly intermediate (Figure 5C). Similar results were obtained by comparing *mhc>dNDUFS5^{RNAi},dNDUFV1^{RNAi}* and *mhc>dNDUFV1^{RNAi}* thoraxes (Figure 5C). Accordingly, we deduce from these results that when dNDUFS5 expression levels are impaired, the transient ~700 kDa assembly intermediate stalls and accumulates, impeding progression of CI biogenesis and ultimately resulting in a bottleneck of the ~550 and ~315 kDa assembly intermediates as well.

To gain further insight into the identity of the ~700 kDa assembly intermediate, a single gel slice encompassing the region shown in Figure 5A was excised from native gels containing samples from wild-type and *mhc>dNDUFS5^{RNAi}* thoraxes. Proteins from the gel slice were digested and analyzed by liquid chromatography (LC) mass spectrometry (MS), and a label-free spectral counting approach was used to generate a heatmap for some of the proteins that showed altered expression levels between the samples. In agreement with our results showing a stalling and accumulation of the ~700 kDa assembly intermediate in this portion of the gel, we observed that several CI subunits were upregulated in the *mhc>dNDUFS5^{RNAi}* sample relative to wild-type (Figure 5D). However, in stark contrast to the other CI subunits, we consistently observed (in six biological replicates taken at different time points of the day to control for circadian regulation) that dNDUFA10 was downregulated in the *mhc>dNDUFS5^{RNAi}* sample, indicating that incorporation of dNDUFS5 into CI is necessary to stabilize or promote incorporation of dNDUFA10 into the complex (Figure 5D). In mammalian systems, at least five CI assembly factors—ECSIT, TMEM126B, NDUFAF1, ACAD9, and TIMMDC1—are typically found associated with CI assembly intermediates and have been dubbed the mitochondrial complex I assembly (MCIA) complex (Guarani et al., 2014; Heide et al., 2012; Nouws et al., 2010; Vogel et al., 2007). We found four of these assembly factors (dECSIT, dNDUFAF1, dACAD9, and dTIMMDC1) associated with the 700 kDa assembly intermediate that were upregulated in the *mhc>dNDUFS5^{RNAi}* samples, further

confirming that it is a true assembly intermediate in CI biogenesis (Figure 5D; Table S4).

The Distal Portion of the Membrane Arm of CI Is Assembled Independently of the Matrix Arm

We noticed that in some instances in which CI assembly was impaired, an additional band accumulated between the CIII and CIV bands in both the Coomassie- and silver-stained gels (arrows in Figures 2A and 2B). A closer examination revealed that the accumulation of this intermediate was more readily evident in samples in which subunits localized to the hydrophilic matrix domain were disrupted (i.e., the dNDUFS, dNDUFV, and dNDUFA subunits) (Figure 1A). In line with our observations described in Figures 3, 4, and 5, we hypothesized that this band was likely another CI assembly intermediate that had stalled and accumulated as a result of a block in CI biogenesis. We decided to identify the constituents of this putative assembly intermediate via MS.

We cut out the region of the gel corresponding to the stalled assembly intermediate in the wild-type, *mhc>dNDUFS5^{RNAi}*, and *mhc>dNDUFV1^{RNAi}* thoraxes (Figure 6A) and used label-free quantification of peptides to ascertain which subunits and possibly assembly factors were altered between the two samples. Several components of the ETC machinery were downregulated, but there was a dramatic increase in CI subunits that are part of the distal membrane domain (i.e., all the dNDUFB subunits as well as dNDUFAB1, dNDUFC2, ND4, and ND5) (Figures 6B and 6C; Table S5). We note that there was no obvious accumulation of this assembly intermediate in blue native or silver-stained gels when any of these subunits (i.e., the dNDUFB subunits or NDUFAB1 and NDUFC2 subunits) were disrupted (Figures 2A and 2B). Notably, many of these membrane-associated subunits were present in the corresponding gel slice from the wild-type samples (although at lower levels). All the components of the MCIA complex (i.e., dECSIT, dNDUFAF1, dACAD9, dTMEM126B, and dTIMMDC1) were also found associated with this assembly intermediate. Based on current assignments of the various CI subunits, this assembly intermediate is clearly the distal portion of the membrane arm (Fiedorczuk et al., 2016; Vinothkumar et al., 2014; Zhu et al., 2016; Zickermann et al., 2015).

Figure 5. Identification of an ~700 kDa Assembly Intermediate of CI in *Drosophila*

- (A) Top: immunoblots of samples obtained from wild-type and *mhc>dNDUFS5^{RNAi}* thoraxes of flies aged for 6 hr after eclosure depicting co-migration of the ~700 kDa intermediate and CV. Left and middle: anti-NDUFS3 antibodies detect the fully assembled CI, the ~700 kDa subcomplex, and other assembly intermediates in *dNDUFS5^{RNAi}* thoraxes. Note that in the middle, the region of the membrane just below CI was cut and imaged. Right: anti-ATPSyn β detects the CV monomer (700 kDa) and dimer as shown. Bottom: mitochondrial protein complexes from wild-type and *mhc>dNDUFS5^{RNAi}* thoraxes were resolved by BN-PAGE, and the region corresponding to the ~700 kDa assembly intermediate (i.e., CV, demarcated) was cut out, subjected to tryptic digestion, and analyzed by label-free quantitative LC-MS/MS.
- (B) Immunoblots from samples obtained after 6, 12, and 24 hr post-eclosure from thoraxes in which NDUFS1, NDUFS3, NDUFS5, and NDUFV1 were knocked down as a result of transgenic RNAi expression. Note that the ~815 kDa assembly intermediate accumulates as a result of disruption of NDUFS1 and NDUFV1, and the ~700 kDa assembly intermediate stalls and accumulates in NDUFS5 mutants at all time points. Importantly, upon prolonged exposure of the immunoblot, a band corresponding to the ~700 kDa assembly intermediate can also be observed in wild-type samples (denoted with the asterisk in the bottom panel), which confirms that it is an authentic, albeit transient assembly intermediate.
- (C) The accumulation of the ~815 kDa assembly intermediate was significantly attenuated in *mhc>dNDUFS5^{RNAi},dNDUFS1^{RNAi}* thoraxes relative to *mhc>dNDUFS1^{RNAi}* thoraxes; instead there is an accumulation of the ~700 kDa assembly intermediate. Similar results were obtained when samples from *mhc>dNDUFS5^{RNAi},dNDUFV1^{RNAi}* thoraxes were compared with samples from *mhc>dNDUFV1^{RNAi}* thoraxes.
- (D) Proteomic changes in the gel slice sample from wild-type and *mhc>dNDUFS5^{RNAi}* thoraxes corresponding to the ~700 kDa assembly intermediate. Relative protein abundance among biological samples is expressed by spectral counts on a log scale. Several CI subunits and CIAFs, most notably components of the MCIA complex, are upregulated in the ~700 kDa assembly intermediate. However, the amount of dNDUFA10 (denoted with an asterisk) is reduced in *mhc>dNDUFS5^{RNAi}* thoraxes relative to wild-type. See Table S4 for all the peptides identified.

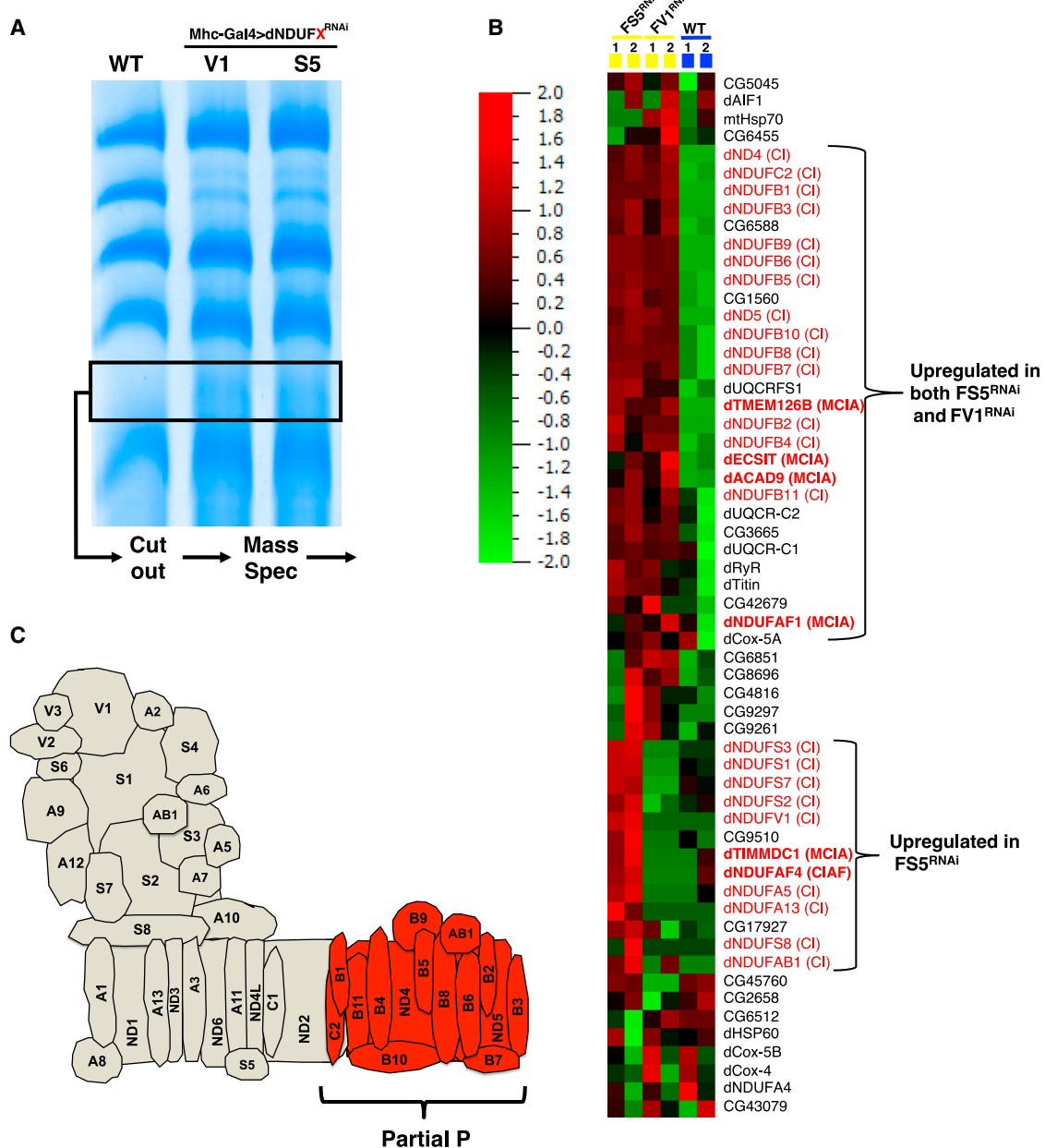


Figure 6. CI Assembly in *Drosophila* Involves an Assembly Intermediate Containing Several Membrane-Associated Accessory Subunits

(A) Mitochondrial protein complexes from wild-type, *mhc>dNDUF^{S5}^{RNAi}*, and *mhc>dNDUFV1^{RNAi}* thoraxes were separated by BN-PAGE, and the region corresponding to the accumulated assembly intermediate (demarcated) was cut out, subjected to tryptic digestion, and analyzed by label-free quantitative LC-MS/MS.

(B) Proteomic changes in the gel slice samples from wild-type, *mhc>dNDUF^{S5}^{RNAi}*, and *mhc>dNDUFV1^{RNAi}* thoraxes. Relative protein abundance among biological samples is expressed by spectral counts on a log scale. The color scale bar indicates the range of protein expression levels. See additional information in Table S5.

(C) Schematic representation highlighting the membrane subunits that are upregulated in the gel slice (shown in red font) from the *mhc>dNDUF^{S5}^{RNAi}* and *mhc>dNDUFV1^{RNAi}* thoraxes.

Proposed Model of CI Assembly in *Drosophila* Muscle

We propose a model for CI assembly in *Drosophila* flight muscles in which dNDUFS2, dNDUFS3, dNDUFS7, dNDUFS8, and dNDUFA5 are combined in essentially one step to form

the Q module, which is anchored to the membrane by dND1 (Figure 7). This assembly intermediate corresponds to the assembly intermediate in mammalian systems that was previously referred to as the ~400 kDa subcomplex but has recently been

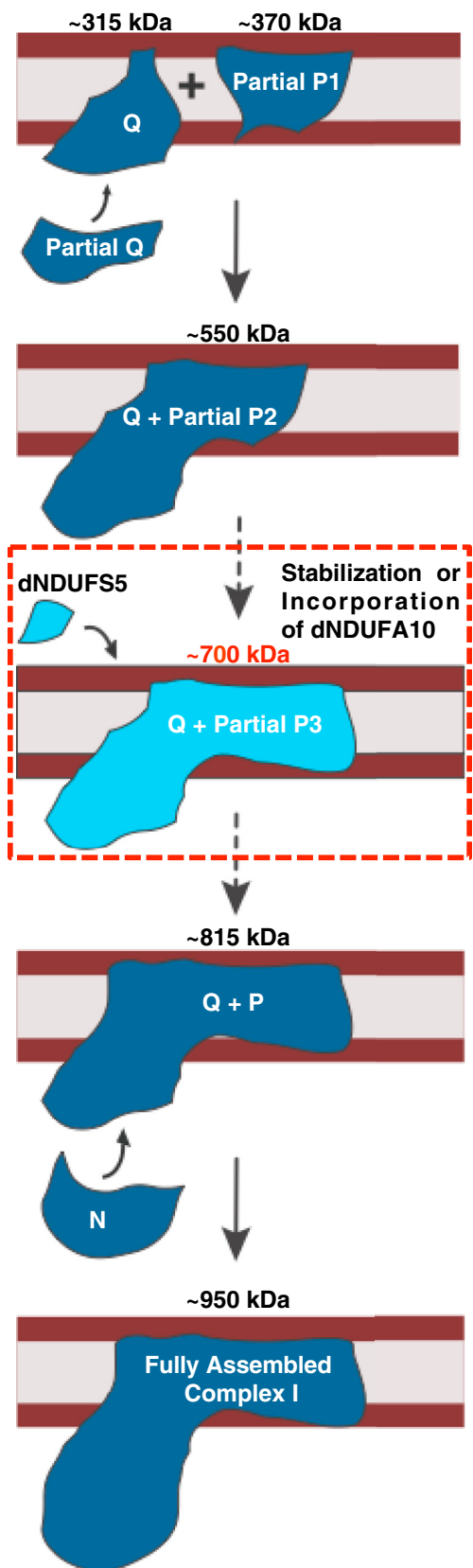


Figure 7. Proposed Model of CI Assembly in *Drosophila* Flight Muscle

An assembly intermediate consisting of dNDUFS2, dNDUS3, dNDUFS7, dNDUFS8, and dNDUFA5 combined in essentially one step to form the Q module, which is anchored to the membrane by ND1. Subsequently, an independently formed subcomplex comprising membrane-associated subunits (partial P1) is conjugated to the Q module, and possibly other subunits, to form an assembly intermediate comprised of the Q module and part of the P module (Q + partial P2). This grows by the addition of more subunits to form a transient assembly intermediate of ~700 kDa (Q + partial P3). We propose that dNDUFS5 is then incorporated at this step, to promote incorporation or stabilization of dNDUFA10. Subsequently, the transient ~700 kDa assembly intermediate is rapidly converted to the ~815 kDa assembly intermediate, consisting of the complete P and Q modules (Q + P). Finally, the N module is added to produce the CI holoenzyme.

re-estimated as the ~315 kDa subcomplex (Andrews et al., 2013; Vartak et al., 2014). This is consistent with the observation that assembly intermediates containing dNDUFS2, dNDUFS3, dNDUFS7, dNDUFS8, and dNDUFA5 co-migrate in blue native gels (Table S2) and that immunoblotting with both anti-ND1 and anti-NDUFS3 detects the ~315 kDa assembly intermediate (Figure 3C).

Subsequently, another assembly intermediate consisting of some of the subunits in the membrane domain is formed. This assembly intermediate comprises part of the P module (i.e., partial P1) and is conjugated to the Q module to form an assembly intermediate that corresponds to the ~550 kDa (formerly ~650 kDa) assembly intermediate previously described in mammalian systems (Figure 7). Although proteomic analyses of the assembly intermediate that accumulates in *mhc>dNDUFS5^{RNAi}* and *mhc>dNDUFA10^{RNAi}* thoraces shows that all the dNDUFB subunits as well as dNDUFC1, dNDUFAB1, ND4, and ND5 subunits are present in the subcomplex (see Table S5), it is unlikely that all the membrane subunits are incorporated into the complex at this stage under normal (wild-type) conditions. We hypothesize that the accumulation of the membrane accessory subunits in response to genetic disruption of the matrix subunits may be a compensatory mitochondrial stress signaling mechanism impinging on the nucleus and resulting in a system that is poised to rapidly resume CI biogenesis if and when the missing matrix subunit becomes available. The accretion of the partial P module under conditions in which other components of the CI assembly machinery are impaired provides further evidence that the various modules of the complex (i.e., the Q, P, and N modules) are assembled largely independently of each other *in vivo*.

The ~550 kDa assembly intermediate grows by the addition of more subunits to form a transient assembly intermediate of ~700 kDa (Figure 7); we postulate that dNDUFS5 is then incorporated at or just prior to this stage together with possibly dNDUFA10 to rapidly convert the ~700 kDa assembly intermediate to the ~815 kDa assembly intermediate, consisting of the complete P and Q modules (Figure 7). Finally, the N module is added to produce the CI holoenzyme (Figure 7).

DISCUSSION

We have exploited the genetic capabilities of *Drosophila* to uncover the mechanism of CI assembly *in vivo* in *Drosophila* flight

muscles. Our immunoblotting and proteomic analyses reveal that during CI assembly in *Drosophila*, the first membrane-bound major assembly intermediate that forms contains at least the following six subunits: dND1, dNDUFS2, dNDUFS3, dNDUFS7, dNDUFS8, and dNDUFA5. On the basis of its constituents and migration pattern in native PAGE, we conclude that this assembly intermediate is the same assembly intermediate traditionally referred to as the ~315 kDa assembly intermediate from studies on mammalian CI assembly and corresponds to the Q module of CI (Andrews et al., 2013; Vartak et al., 2014). Consistent with their roles in regulating formation of the Q module, we found that genetic disruption of dNDUFS2, dNDUFS3, dNDUFA5, and dNDUFS7 attenuated the amount of the ~315 kDa assembly intermediate formed.

Unexpectedly, we found an ~700 kDa assembly intermediate that is short-lived (at least relative to the ~315, ~550, and ~815 kDa assembly intermediates), as it is rapidly converted into the ~815 kDa assembly intermediate. Importantly, our proteomic analyses revealed that incorporation of dNDUFS5 into CI around this stage is necessary to stabilize or promote incorporation of dNDUFA10 into the complex. Similar to the ~315, ~550, and ~815 kDa assembly intermediates, the ~700 kDa subcomplex is a true assembly intermediate, as it can be detected in wild-type muscles as well. Additionally, components of the MCIA complex are associated with the ~700 kDa assembly intermediate, as has been reported for other assembly intermediates observed in mammalian systems. RNAi-mediated disruption of dNDUFS5 led to a stalling and accumulation of this otherwise transient assembly intermediate, to a point at which it is readily detectable by western blots, most likely because this is the stage at or around which dNDUFS5 is incorporated into the complex.

It is possible that mutations in some accessory subunits will have both primary and secondary effects. As a case in point, dNDUFS5 disruption may first impair conversion of the ~700 kDa assembly intermediate to the ~815 kDa assembly intermediate and consequently impair CI assembly (as we have shown), but ultimately, the accumulation of the ~700 kDa assembly intermediate can activate the mitochondrial unfolded protein response as well as other stress signaling cascades, with far-reaching consequences (Haynes et al., 2013; Jensen and Jasper, 2014; Owusu-Ansah and Banerjee, 2009; Owusu-Ansah et al., 2008, 2013). As another example, when dNDUFB3 was disrupted, no specific assembly intermediates were stalled or disintegrated. Instead, there was a general reduction in the level of expression of all assembly intermediates. It is possible that disruption of dNDUFB3 activates stress signaling pathways that induce apoptosis or culminate in a general reduction of protein synthesis, leading to a reduction in CI assembly.

We find that at least 42 of the 44 distinct human CI proteins are conserved in *Drosophila*. The two human CI proteins for which a clear ortholog was not readily identified in *Drosophila* by DIOPT are NDUFA3 (9 kDa) and NDUFC1 (6 kDa), which are two of the smallest subunits of the complex. Interestingly, obvious orthologs of NDUFC1 are not found in *C. elegans* or *Yarrowia lipolytica*, and the orthologs in vertebrates such as zebrafish and *Xenopus* have very weak homology (DIOPT score of 1) to the human

protein. Therefore it is possible that this subunit has significant sequence diversion in *Drosophila* and although present was not recognized by DIOPT. For most of the CI subunits in which multiple paralogs were identified by DIOPT (i.e., NDUFS2, NDUFS7, NDUFV2, NDUFA7, and NDUFB2), only one of the paralogs was detected as a bona fide CI subunit in flight muscles. However, as an exception to this general rule, two of the three paralogs of NDUFV1 were detected as part of CI in skeletal muscles via MS. ND-51 (CG9140) appears to be the authentic ortholog of human NDUFV1, as it is highly expressed in skeletal muscles relative to ND-51L (CG11423) and is comparable in size to the human ortholog (both are about 51 kDa). ND-51L is a 77 kDa protein with a stretch of about 200 amino acids at the N terminus that is not present in either the *Drosophila* paralog (ND-51) or human ortholog (NDUFV1). It remains to be determined whether the expression of the subunits with multiple paralogs are regulated in a tissue-specific manner to generate mitochondria with varied CI activities or whether they are regulated in the same tissue in response to different environmental conditions to fine-tune the activity of CI.

In summary, we have described the mechanism of CI assembly in *Drosophila* flight muscles and defined specific roles for some of the accessory subunits in CI assembly. Importantly, although CI dysfunction has been implicated in a large number of pathologies, we find that knocking down the expression of various antioxidant enzymes or mitochondrial protein quality control genes does not solely impair CI assembly, indicating that destabilization of CI may not be the sole underlying factor in many mitochondrial disorders (Figure S4). In addition, our proteomic analyses established that incorporation of dNDUFS5 into CI is necessary to stabilize or promote incorporation of dNDUFA10 into the complex. We note that our analyses of CI assembly in an in vivo setting, in which CI biogenesis is subject to both developmental and environmental cues, revealed that many of the accessory subunits are required for both assembly and viability. Moreover, several NDUFB subunits (dNDUFB1, dNDUFB4, dNDUFB5, dNDUFB6, and dNDUFB10) seem to regulate the stability of the 315 kDa assembly intermediate, in apparent deviation from what will be expected from current models of mammalian CI assembly. However, the mechanism of CI biogenesis in *Drosophila* flight muscles is remarkably similar to what has been described in mammalian systems, and the differences observed here may be due to the fact that we have analyzed CI assembly in an in vivo setting. Accordingly, *Drosophila* is a suitable organism for addressing questions relevant to mammalian CI biogenesis. We anticipate that future studies using the full repertoire of genetic tools and resources in *Drosophila* should foster the discovery of paradigms for regulating CI assembly in humans.

EXPERIMENTAL PROCEDURES

Drosophila Strains and Genetics

For a list of stocks used and detailed experimental procedures, see [Supplemental Experimental Procedures](#).

BN-PAGE

BN-PAGE was performed using NativePAGE gels from Life Technologies, following the manufacturer's instructions.

Silver Staining

Silver staining of native gels was performed with the SilverXpress staining kit from Life Technologies, following the manufacturer's protocol.

In-Gel CI Activity

CI activity in native gels was assayed by incubating the native gels in 0.1 mg/ml NADH, 2.5 mg/ml nitrotetrazolium blue chloride, and 5 mM Tris-HCl (pH 7.4) at room temperature.

Immunoblotting

For immunoblotting of samples in native gels, protein complexes from native gels were transferred to polyvinylidene fluoride (PVDF) membranes (Bio-Rad) and probed with the relevant antibodies using standard procedures.

MS Analyses

After MS with a Thermo Fusion Tribrid mass spectrometer, tandem mass spectra from raw files were searched against a *Drosophila* protein database using the Proteome Discoverer 1.4 software (Thermo Finnigan). The Proteome Discoverer application extracts relevant MS/MS spectra from the .raw file and determines the precursor charge state and the quality of the fragmentation spectrum. The Proteome Discoverer probability-based scoring system rates the relevance of the best matches found by the SEQUEST algorithm. The *Drosophila* protein database was downloaded as FASTA-formatted sequences from Uniprot protein database (database released in May 2015). The peptide mass search tolerance was set to 10 ppm. A minimum sequence length of seven amino acids residues was required. Only fully tryptic peptides were considered. To calculate confidence levels and false discovery rates (FDR), Proteome Discoverer generates a decoy database containing reverse sequences of the non-decoy protein database and performs the search against this concatenated database (non-decoy + decoy). Scaffold (Proteome Software) was used to visualize searched results. The discriminant score was set at less than 1% FDR determined on the basis of the number of accepted decoy database peptides to generate protein lists for this study. Spectral counts were used for estimation of relative protein abundance between samples.

SUPPLEMENTAL INFORMATION

Supplemental Information includes Supplemental Experimental Procedures, four figures, and five tables and can be found with this article online at <http://dx.doi.org/10.1016/j.celrep.2017.06.015>.

AUTHOR CONTRIBUTIONS

E.O.-A. conceived the project, designed experiments, and secured funding for the work. C.J.G., J.K., E.C., and E.O.-A. performed all experiments, except mass spectrometry. E.I.C. performed mass spectrometry. E.O.-A., C.J.G., J.K., and E.I.C. analyzed and discussed results. E.O.-A. wrote the manuscript with feedback from E.I.C. C.J.G., and J.K.

ACKNOWLEDGMENTS

We thank members of the Owusu-Ansah lab for general discussions; Eric Schon, Estela Area-Gomez, Henry Colecraft, Barbara Corneo, Wes Grueber, Laura Johnston, Richard Kitsis, Andrew Marks, Martin Picard, Liza Pon, Mimi Shirasu-Hiza, and David Walker for fly stocks, reagents, and critical discussions; and Stavroula Kousteni for critical discussions and for providing skeletal and cardiac muscle samples from mice. We acknowledge the Bloomington *Drosophila* Stock Center, the National Institute of Genetics (Japan), and the Vienna *Drosophila* Resource Center for various fly strains. We appreciate Steven Shikhe's technical assistance in dissecting cardiac and skeletal muscles from mice and the technical assistance obtained from the Proteomics Shared Resource at the Herbert Irving Comprehensive Cancer Center, Columbia University Medical Center. This work was supported by an Institutional Cardiovascular Research Training Grant (T32 HL120826) to C.J.G. and J.K. and a NIH R21 grant (DK112074), a pilot grant from the Robert N. Butler

Columbia Aging Center, and institutional startup funds from the Department of Physiology and Cellular Biophysics, Columbia University Medical Center, to E.O.-A.

Received: December 19, 2016

Revised: May 18, 2017

Accepted: June 1, 2017

Published: July 5, 2017

REFERENCES

- Abdrakhmanova, A., Zwicker, K., Kerscher, S., Zickermann, V., and Brandt, U. (2006). Tight binding of NADPH to the 39-kDa subunit of complex I is not required for catalytic activity but stabilizes the multiprotein complex. *Biochim. Biophys. Acta* **1757**, 1676–1682.
- Andrews, B., Carroll, J., Ding, S., Fearnley, I.M., and Walker, J.E. (2013). Assembly factors for the membrane arm of human complex I. *Proc. Natl. Acad. Sci. U.S.A.* **110**, 18934–18939.
- Balsa, E., Marco, R., Perales-Clemente, E., Szklarczyk, R., Calvo, E., Landáuri, M.O., and Enriquez, J.A. (2012). NDUFA4 is a subunit of complex IV of the mammalian electron transport chain. *Cell Metab.* **16**, 378–386.
- Berger, I., Hershkovitz, E., Shaag, A., Edvardson, S., Saada, A., and Elpeleg, O. (2008). Mitochondrial complex I deficiency caused by a deleterious NDUFA11 mutation. *Ann. Neurol.* **63**, 405–408.
- Brand, A.H., and Perrimon, N. (1993). Targeted gene expression as a means of altering cell fates and generating dominant phenotypes. *Development* **118**, 401–415.
- Budde, S.M., van den Heuvel, L.P., Janssen, A.J., Smeets, R.J., Buskens, C.A., DeMeirlier, L., Van Coster, R., Baethmann, M., Voit, T., Trijbels, J.M., and Smeitink, J.A. (2000). Combined enzymatic complex I and III deficiency associated with mutations in the nuclear encoded NDUFS4 gene. *Biochem. Biophys. Res. Commun.* **275**, 63–68.
- Clason, T., Ruiz, T., Schägger, H., Peng, G., Zickermann, V., Brandt, U., Michel, H., and Radermacher, M. (2010). The structure of eukaryotic and prokaryotic complex I. *J. Struct. Biol.* **169**, 81–88.
- Duarte, M., Sousa, R., and Videira, A. (1995). Inactivation of genes encoding subunits of the peripheral and membrane arms of neurospora mitochondrial complex I and effects on enzyme assembly. *Genetics* **139**, 1211–1221.
- Efremov, R.G., Baradaran, R., and Sazanov, L.A. (2010). The architecture of respiratory complex I. *Nature* **465**, 441–445.
- Fiedorczuk, K., Letts, J.A., Degliesposti, G., Kaszuba, K., Skehel, M., and Sazanov, L.A. (2016). Atomic structure of the entire mammalian mitochondrial complex I. *Nature* **538**, 406–410.
- Guarani, V., Paulo, J., Zhai, B., Huttlin, E.L., Gygi, S.P., and Harper, J.W. (2014). TIMMDC1/C3orf1 functions as a membrane-embedded mitochondrial complex I assembly factor through association with the MCIA complex. *Mol. Cell. Biol.* **34**, 847–861.
- Guerrero-Castillo, S., Baertling, F., Kownatzki, D., Wessels, H.J., Arnold, S., Brandt, U., and Nijtmans, L. (2017). The assembly pathway of mitochondrial respiratory chain complex I. *Cell Metab.* **25**, 128–139.
- Haynes, C.M., Fiorese, C.J., and Lin, Y.F. (2013). Evaluating and responding to mitochondrial dysfunction: the mitochondrial unfolded-protein response and beyond. *Trends Cell Biol.* **23**, 311–318.
- Heide, H., Bleier, L., Steger, M., Ackermann, J., Dröse, S., Schwamb, B., Zörnig, M., Reichert, A.S., Koch, I., Wittig, I., and Brandt, U. (2012). Complexome profiling identifies TMEM126B as a component of the mitochondrial complex I assembly complex. *Cell Metab.* **16**, 538–549.
- Hirst, J. (2013). Mitochondrial complex I. *Annu. Rev. Biochem.* **82**, 551–575.
- Hoefs, S.J., Dieteren, C.E., Distelmaier, F., Janssen, R.J., Epplen, A., Swarts, H.G., Forkink, M., Rodenburg, R.J., Nijtmans, L.G., Willems, P.H., et al. (2008). NDUFA2 complex I mutation leads to Leigh disease. *Am. J. Hum. Genet.* **82**, 1306–1315.

- Hoefs, S.J., van Spronsen, F.J., Lenssen, E.W., Nijtmans, L.G., Rodenburg, R.J., Smeitink, J.A., and van den Heuvel, L.P. (2011). NDUFA10 mutations cause complex I deficiency in a patient with Leigh disease. *Eur. J. Hum. Genet.* **19**, 270–274.
- Hu, Y., Flockhart, I., Vinayagam, A., Bergwitz, C., Berger, B., Perrimon, N., and Mohr, S.E. (2011). An integrative approach to ortholog prediction for disease-focused and other functional studies. *BMC Bioinformatics* **12**, 357.
- Jensen, M.B., and Jasper, H. (2014). Mitochondrial proteostasis in the control of aging and longevity. *Cell Metab.* **20**, 214–225.
- Kirby, D.M., Salemi, R., Sugiana, C., Ohtake, A., Parry, L., Bell, K.M., Kirk, E.P., Boneh, A., Taylor, R.W., Dahl, H.H., et al. (2004). NDUFS6 mutations are a novel cause of lethal neonatal mitochondrial complex I deficiency. *J. Clin. Invest.* **114**, 837–845.
- Nehls, U., Friedrich, T., Schmiede, A., Ohnishi, T., and Weiss, H. (1992). Characterization of assembly intermediates of NADH:ubiquinone oxidoreductase (complex I) accumulated in *Neurospora* mitochondria by gene disruption. *J. Mol. Biol.* **227**, 1032–1042.
- Nouws, J., Nijtmans, L., Houten, S.M., van den Brand, M., Huynen, M., Venselaar, H., Hoefs, S., Goerich, J., Kronick, J., Hutchin, T., et al. (2010). Acyl-CoA dehydrogenase 9 is required for the biogenesis of oxidative phosphorylation complex I. *Cell Metab.* **12**, 283–294.
- Ostergaard, E., Rodenburg, R.J., van den Brand, M., Thomsen, L.L., Duno, M., Batbayli, M., Wibrand, F., and Nijtmans, L. (2011). Respiratory chain complex I deficiency due to NDUFA12 mutations as a new cause of Leigh syndrome. *J. Med. Genet.* **48**, 737–740.
- Owusu-Ansah, E., and Banerjee, U. (2009). Reactive oxygen species prime *Drosophila* hematopoietic progenitors for differentiation. *Nature* **461**, 537–541.
- Owusu-Ansah, E., Yavari, A., Mandal, S., and Banerjee, U. (2008). Distinct mitochondrial retrograde signals control the G1-S cell cycle checkpoint. *Nat. Genet.* **40**, 356–361.
- Owusu-Ansah, E., Song, W., and Perrimon, N. (2013). Muscle mitohormesis promotes longevity via systemic repression of insulin signaling. *Cell* **155**, 699–712.
- Radermacher, M., Ruiz, T., Clason, T., Benjamin, S., Brandt, U., and Zickermann, V. (2006). The three-dimensional structure of complex I from *Yarrowia lipolytica*: a highly dynamic enzyme. *J. Struct. Biol.* **154**, 269–279.
- Rera, M., Bahadorani, S., Cho, J., Koehler, C.L., Ulgherait, M., Hur, J.H., Ansari, W.S., Lo, T., Jr., Jones, D.L., and Walker, D.W. (2011). Modulation of longevity and tissue homeostasis by the *Drosophila* PGC-1 homolog. *Cell Metab.* **14**, 623–634.
- Roy, S., and VijayRaghavan, K. (1999). Muscle pattern diversification in *Drosophila*: the story of imaginal myogenesis. *BioEssays* **21**, 486–498.
- Scacco, S., Petruzzella, V., Budde, S., Vergari, R., Tamborra, R., Panelli, D., van den Heuvel, L.P., Smeitink, J.A., and Papa, S. (2003). Pathological mutations of the human NDUFS4 gene of the 18-kDa (AQDQ) subunit of complex I affect the expression of the protein and the assembly and function of the complex. *J. Biol. Chem.* **278**, 44161–44167.
- Stroud, D.A., Surgenor, E.E., Formosa, L.E., Reljic, B., Frazier, A.E., Dibley, M.G., Osellame, L.D., Stait, T., Beilharz, T.H., Thorburn, D.R., et al. (2016). Accessory subunits are integral for assembly and function of human mitochondrial complex I. *Nature* **538**, 123–126.
- Tuschen, G., Sackmann, U., Nehls, U., Haiker, H., Buse, G., and Weiss, H. (1990). Assembly of NADH: ubiquinone reductase (complex I) in *Neurospora* mitochondria. Independent pathways of nuclear-encoded and mitochondrially encoded subunits. *J. Mol. Biol.* **213**, 845–857.
- Vartak, R.S., Semwal, M.K., and Bai, Y. (2014). An update on complex I assembly: the assembly of players. *J. Bioenerg. Biomembr.* **46**, 323–328.
- Vinothkumar, K.R., Zhu, J., and Hirst, J. (2014). Architecture of mammalian respiratory complex I. *Nature* **515**, 80–84.
- Vogel, R.O., Janssen, R.J., van den Brand, M.A., Dieteren, C.E., Verkaart, S., Koopman, W.J., Willemse, P.H., Pluk, W., van den Heuvel, L.P., Smeitink, J.A., and Nijtmans, L.G. (2007). Cytosolic signaling protein Ecsit also localizes to mitochondria where it interacts with chaperone NDUFAF1 and functions in complex I assembly. *Genes Dev.* **21**, 615–624.
- Wittig, I., Braun, H.P., and Schägger, H. (2006). Blue native PAGE. *Nat. Protoc.* **1**, 418–428.
- Zhu, J., Vinothkumar, K.R., and Hirst, J. (2016). Structure of mammalian respiratory complex I. *Nature* **536**, 354–358.
- Zickermann, V., Wirth, C., Nasiri, H., Siegmund, K., Schwalbe, H., Hunte, C., and Brandt, U. (2015). Structural biology. Mechanistic insight from the crystal structure of mitochondrial complex I. *Science* **347**, 44–49.